PLASTICITY AND ROUGHNESS INDUCED CLOSURE IN AGED HARDENED ALUMINIUM ALLOYS

L. P. Borrego[1*], J. M. Ferreira[2] and J. M. Costa[2]

[1] Dep. of Mechanical Engineering, ISEC/IPC, 3030 Coimbra, Portugal
[2] Dep. of Mechanical Engineering/FCT, University of Coimbra, Portugal

ABSTRACT: *Fatigue crack propagation tests in constant amplitude loading, as well as with single peak overloads, have been performed in 6082-T6 aluminium alloys with different Mn and Cr contents. All experiments were performed, either in load control or in constant ΔK conditions, using MT specimens in a servohydraulic machine at a frequency of 20 Hz. Crack closure was monitored in all tests by the compliance technique using a pin microgauge. Surface roughness profiles were obtained and related with crack closure and crack growth rates. A moderate R-ratio and a strong material dependence effects on the fatigue crack growth were observed. These effects are discussed in terms of the different dominant closure mechanism (plasticity-induced closure or roughness-induced closure). When roughness-induced closure is the prime pre-overload closure mechanism the retardation effect is decreased in comparison to when plasticity-induced closure is dominant.*

INTRODUCTION

Age hardened aluminium alloys are of great technological importance. In particular for ground transport systems, when relatively high strength, good corrosion resistance and high toughness are required in conjunction with good formability and weldability, aluminium alloys with Mg and Si as alloying elements are used (Al-Mg-Si / 6xxx series).

Constant amplitude fatigue crack growth in Al-Mg-Si alloys can be highly influenced by the dispersoid content due to Mn or Cr being present [1-3] as well as by the type of age hardening heat-treatment [3-5]. In all cases the crack growth behaviour depends mainly on whether an alloy shows plasticity-induced closure only, or additionally other retarding mechanisms such as roughness-induced closure [1-4].

---

* Corresponding author. e-mail: luis.borrego@dem.uc.pt,

Several mechanisms have been proposed to explain crack growth retardation following single peak tensile overloads, which include models based on residual stress, crack closure, crack tip blunting, strain hardening, crack branching and reversed yielding. The precise micromechanisms responsible for these phenomena are not fully understood.

The present paper analyses the influence of the dominant closure mechanism (plasticity-induced or roughness-induced) in constant and variable-amplitude fatigue crack growth.

EXPERIMENTAL DETAILS

This research was conduced using an AlMgSi1 (6082) aluminium alloy with a T6 heat treatment has received. The chemical composition and the mechanical properties are shown in tables 1 and 2, respectively. The data presented in these tables are for the alloy tested in this work (alloy B) and also for an alloy analysed in previous work (alloy A) [6,7]. The alloys A and B differ mainly in the manganese and chromium contents.

TABLE 1: Chemical composition of the 6082-T6 alloys [% Weight].

Alloy	Si	Mg	Mn	Fe	Cr	Cu	Zn	Ti	Other
A	1.05	0.80	0.68	0.26	0.01	0.04	0.02	0.01	
B	0.98	1.08	0.90	0.32	0.25	0.07	0.15	0.10	0.15

TABLE 2: Mechanical properties of the 6082-T6 alloys.

Alloy	Tensile strength, σ_{UTS} [MPa]	Yield strength, σ_{YS} [MPa]	Elongation, ε_r [%]
A	300±2.5	245±2.7	9
B	290±1.9	250±2.4	12

Fatigue tests were conducted, in agreement with the ASTM E647 standard, using Middle-Tension, M(T), 3 mm (alloy A) and 6 mm (alloy B) thick specimens with 200 mm and 50 mm length and width, respectively. The specimens were obtained in the longitudinal transverse (LT) direction

from a laminated plate. The geometry of the M(T) specimen used in this study was presented elsewhere [6].

All experiments were performed in a servohydraulic, closed-loop mechanical test machine with 100 kN capacity, interfaced to a computer for machine control and data acquisition. All tests were conducted in air and room temperature, at a frequency of 20 Hz and a stress ratio of 0.05 or 0.25. The specimens were clamped by hydraulic gripes. The crack length was measured using a travelling microscope (45X) with an accuracy of 10 μm.

The constant amplitude tests where performed in load control. The fatigue crack growth rate data were generated using the K-increasing procedure for $da/dN > 1 \times 10^{-5}$ mm/cycle and the K-decreasing procedure for $da/dN < 1 \times 10^{-5}$ mm/cycle. Crack growth rates were determined by the incremental polynomial method using five consecutive points. The single tensile overload tests were performed under constant ΔK and stress ratio R conditions, by manually shedding the load with crack growth. The load shedding intervals were chosen so that the maximum ΔK_{BL} variation was smaller than 2%. The overloads were applied under load control during one cycle by programming the increase in load to the designated overload value. The crack growth rates were determined by the secant method.

Load-displacement behaviour was monitored at specific intervals throughout each of the tests using a pin microgauge. The gauge pins were placed in the centre of the notch. In order to collect as many load-displacement data as possible during a particular cycle, the frequency was reduced to 0.5 Hz. Noise on the strain gauge output was reduced by passing the signal through a 1 Hz low-pass mathematical filter.

RESULTS AND DISCUSSION

Constant amplitude loading
The influence of the stress ratio on the fatigue crack growth rate for both alloys can be seen in figure 1. The results obtained by Shercliff and Fleck [8] for the alloy 6082-T6, using M(T) and bending specimens with a thickness of 9.9 mm, are also shown in figure 1 for comparison. A moderate *R*-ratio effect on da/dN was observed. The crack growth rate increases with R; this trend is more pronounced for alloy B than for alloy A. Crack growth rates for alloy B are significantly lower than for alloy A, and even lower than the ones obtained in [8]. This behaviour cannot be correlated with the different specimen thickness because as the thickness increases plasticity induced closure tends to be lower and consequently *da/dN* increases [9].
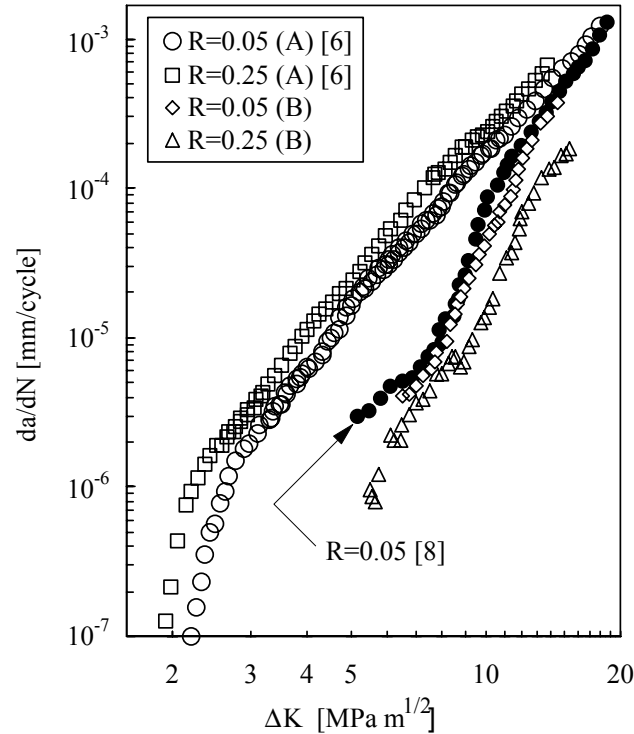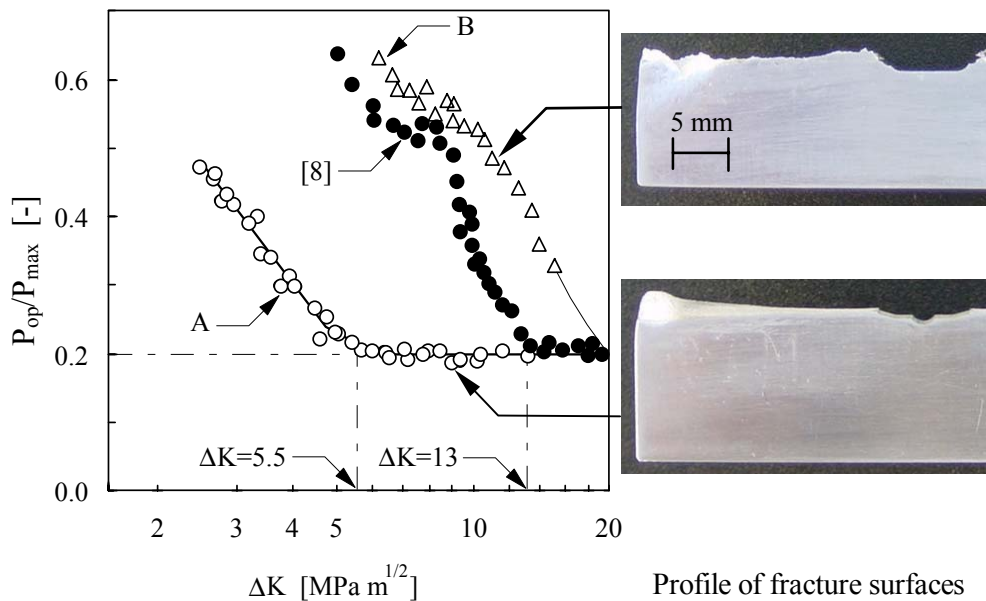
Figure 1: Fatigue crack growth rates for 6082-T6 aluminium alloys.

Figure 2 presents the variation of K_{op}/K_{max} as a function of ΔK for R=0.05. Once again the results obtained by Shercliff and Fleck [8] are shown for comparison. This figure shows that the crack closure data are in accordance with the observed variation in the crack growth rates presented in figure 1, *i.e.*, higher closure levels for lower da/dN values. Indeed, the fatigue crack growth rate data obtained for alloy B for both stress ratios of 0.05 and 0.25, as well as the results of Shercliff and Fleck [8], tend to fall within a narrow scatter band when da/dN is plotted against ΔK_{eff}. Furthermore, this scatter band is in fairly agreement with the da/dN- ΔK_{eff} relationship determined in previous work for alloy A (R=-0.25, 0.05, 0.25 and 0.4) [6]. Therefore, crack closure by itself permits the reduction of all the da/dN-ΔK curves to a unique curve da/dN-ΔK_{eff} independent of the stress ratio R and microstructure once crack closure is compensated for.

Figure 2 also shows that in general K_{op}/K_{max} decreases steeply as ΔK increases until a minimum K_{op}/K_{max} value of approximately 0.21 is attained, after which this ratio remains basically constant. For alloy A and for the data presented in [8] the constant K_{op}/K_{max} ratio is achieved at

$\Delta K=5.5 \text{ MPa m}^{1/2}$ and $\Delta K=13 \text{ MPa m}^{1/2}$, respectively. Such behaviour is due to the dominance of oxide-induced and roughness-induced crack closure for lower ΔK values. For higher values of ΔK plasticity-induced crack closure dominates and closure values are generally independent of ΔK. For alloy B this condition was not attained. From the trend of the curve for this alloy, $K_{op}/K_{max}=0.21$ is estimated to occur only after $\Delta K=20 \text{ MPa m}^{1/2}$. Therefore, it is suggested that different mechanisms of closure must be present in the alloys. For alloy A roughness and plasticity-induced crack closure must be present, being the last significant only for the higher ΔK values. For alloy B roughness-induced closure must dominate in all the range of ΔK values analysed. Images of typical crack profiles for both alloys are also shown in figure 2. It can be seen that alloy B has a more irregular crack profile than alloy A. The roughness of the specimen surfaces was also evaluated. These measurements shown that for alloy B the mean and maximum roughness were typically 3 and 5 times higher, respectively, in comparison with alloy A, which justifies the higher crack closure level observed.

Profile of fracture surfaces

Figure 2: Crack closure data and profiles of fracture surfaces for 6082-T6 alloys. R=0.05

Although, some influence of the age hardening heat-treatment cannot be discharge, the lower crack growth rates observed for alloy B are mainly attributed to the higher dispersoid contend in this alloy (see table 1). The

dispersoid phase is composed by spherical and rod shaped particles, rich in Mn and containing other alloying elements such as Si and Cr, dispersed uniformly in the matrix [3]. This phase promotes planar slip and large deviations of the crack from the average crack growth direction resulting in a tortuous crack path [2,3]. This effect enhances roughness-induced crack closure [2] and, thus, improves the fatigue crack growth properties.

Single peak overload
The normalised crack growth rate, $(da/dN)/(da/dN)_{CA}$, where $(da/dN)_{CA}$ is the constant amplitude crack growth rate corresponding to the baseline level, following a 100 % single tensile overload applied at $\Delta K_{BL}=8$ MPa m$^{1/2}$ can be seen in figure 3. The corresponding crack closure response is presented in figure 4. Figure 3 shows that the overload retardation effect is much higher in alloy A than in alloy B (retardation during approximately a-a_{OL}=7 mm for A, while during only 0.52 mm for B). The crack growth transients in alloy A are in accordance with the behaviour usually referred to as *delayed retardation of crack growth* [10] typically observed for this alloy [6,7]. Alloy B presents mainly an immediate retardation, followed by an increase in the crack growth rate until a maximum value higher than the da/dN value prior to the overload is reached. Only then the crack growth rate gradually approaches the level of the baseline steady state. The initial brief acceleration is only due to the overload cycle itself.

For alloy A, although the pre-overload value is not attained due to the discontinuous closure phenomenon [11] generally seen in this alloy [6,7], the crack closure data show basically the same trend as the experimentally observed crack growth rate response. For Alloy B the closure transients are quite different from the crack growth rate trend. This behaviour is due to the high pre-overload closure level observed for this alloy. It is important to notice that this level is approximately equal to maximum closure induced by the overload applied in alloy A (see fig. 4). Thus, it is suggested that for alloy B the overload cycle induces crack tip blunting, which tends to decrease roughness-induced closure by reducing asperity contact. Additionally, the increase in plasticity-induced closure due to the overload plastic zone is not able to compensate this reduction and, consequently, the crack growth rate increases after the initial retardation. Therefore, plasticity-induced closure, contrary to the observed for alloy A [7], is not the main mechanism responsible for the retardation phase in alloy B. In this alloy other mechanisms must be active, namely, crack tip blunting [12] and/or strain hardening [13].
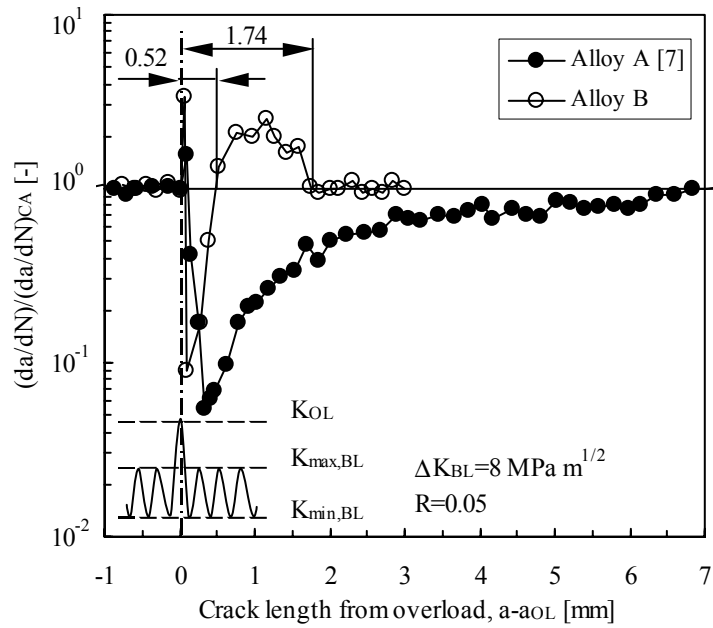
Figure 3: Transient crack growth rate following a single tensile overload.
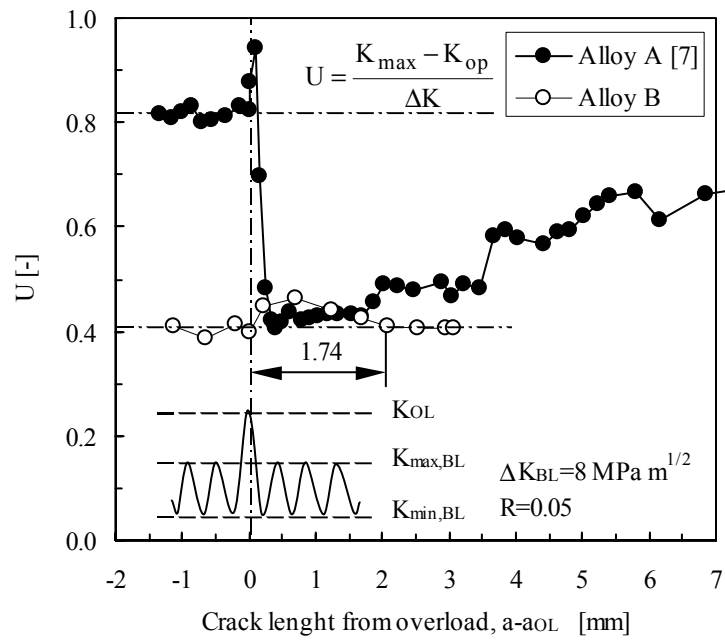
Figure 4: Crack closure response following a single tensile overload.

CONCLUSIONS

1. A moderate *R*-ratio and a strong material dependence effects on the fatigue crack growth were observed. These effects are related to the different closure levels.

2. The crack growth behaviour of 6082-T6 aluminium alloys depends mainly on whether the dominant closure mechanism is plasticity-induced or roughness-induced.

3. When roughness-induced closure is the prime pre-overload closure mechanism, the retardation effect seems to be due to mechanisms other than plasticity-induced closure.

REFERENCES

1. Scheffel R. and Detert K. (1984) *Proc. of ECF5*, Lisboa, Portugal, 805.
2. Scheffel R. and Detert K. (1986) *Proc. of ECF6*, Amsterdam, The Netherlands, 1511.
3. Lee D.H., Park J.H. and Nam S.W. (1999). *Mater Sci Technol* **15**, 450.
4. Bergner F., Zouhar G. and Tempus G. (2001), *Int J Fatigue* **23**, 383.
5. Bergner F. and Zouhar G. (2000), *Int J Fatigue* **22**, 229.
6. Borrego, L.P., Ferreira, J.M. and Costa, J.M. (2001) *Fatigue Fract Engng Mater Struct* **24**, 255.
7. Borrego, L.P., Ferreira, J.M., Pinho da Cruz J.M. and Costa, J.M. (2002) *Engng Fract Mech*, in press.
8. Shercliff, H. R. and Fleck, N. A. (1990) *Fatigue Fract Engng Mater Struct* **13**, 297.
9. Kim J.K., Shim D.S. (2000) *Int J Fatigue*, **22**, 611.
10. Shin, C.S. and Hsu, S.H. (1993) *Int J Fatigue* **15**, 181.
11. Fleck, N.A. (1988). In: *Basic Questions in Fatigue: Volume 1, STP 924*, pp. 157-183, Fong J.T. and Fields R.J. (Ed.). ASTM, Philadelphia.
12. Christensen, R. H. (1959) *Metal Fatigue*. MacGraw-Hill, New York.
13. Jones, R. E. (1973) *Engng Fract Mech* **5**, 585.